Journal of Applied Physics

RESEARCH ARTICLE | AUGUST 01 2008

$P-Zn_3P_2$ single nanowire metal-semiconductor field-effect transistors

C. Liu; L. Dai; R. M. Ma; W. Q. Yang; G. G. Qin

J. Appl. Phys. 104, 034302 (2008)
https://doi.org/10.1063/1.2960494

JOURNAL OF APPLIED PHYSICS **104**, 034302 (2008)

P–Zn_3P_2 single nanowire metal-semiconductor field-effect transistors

C. Liu,[1] L. Dai,[1,a)] R. M. Ma,[1] W. Q. Yang,[1] and G. G. Qin[1,2,a)]
[1]*Department of Physics and State Key Laboratory for Mesoscopic Physics, Peking University, Beijing 100871, People's Republic of China*
[2]*Institute of Optoelectronic Materials and Technology, School of Information Photoelectric Science and Technology, South China Normal University, Guangdong 510631, People's Republic of China*

(Received 19 February 2008; accepted 30 May 2008; published online 1 August 2008)

As far as we know, all the single nanowire (NW) metal-semiconductor field-effect transistors (MESFETs) reported are based on *n*-type NWs. We report MESFETs based on *p*-type Zn_3P_2 single NWs in this paper. The *p*-type Zn_3P_2 single NW MESFETs operate in the enhancement mode (*E*-mode). The source-drain current decreases with gate bias (V_G) increasing, confirming the *p*-type conductance of the Zn_3P_2 NWs. Typically, the *p*-type Zn_3P_2 single NW MESFET has an on/off current ratio of 10^3, a threshold gate voltage of -0.4 V, and a maximum transconductance of 110 nS. © *2008 American Institute of Physics*. [DOI: 10.1063/1.2960494]

I. INTRODUCTION

Semiconductor nanowires (NWs) are good building blocks for functional nanodevices, including the field-effect transistors (FETs), waveguides, photoconductive optical switches, sensors, light-emitting diodes, etc.[1–10] Metal-insulator-semiconductor field-effect transistors (MISFETs) (Refs. 11–17) and metal-semiconductor field-effect transistors (MESFETs) based on single NWs have been reported.[18–20] For wide applications of NW-FETs, both *n*- and *p*-channel are required. For example, complementary logic gate, which has a key characteristic of low static power dissipation and is especially superior in denser circuit integration, involves both *n*- and *p*-channel transistors. However, as far as we know, all the single NW MESFETs reported are based on *n*-type single NWs. In this paper, we report single NW MESFETs based on *p*-type Zn_3P_2 single NWs. The *p*-type Zn_3P_2 single NW MESFETs operate in the enhancement mode (*E*-mode). *E*-mode (normally off) FETs do not have a conductive channel at zero gate voltage, and have an advantage in high speed and low power consumption operation devices.[19]

II. EXPERIMENTS

The *p*-type Zn_3P_2 NWs were synthesized via the chemical-vapor deposition method in a tube furnace (the details were presented in Ref. 21). We used a mixture of Zn (99.99%) powders and InP (99.99%) fragments (with mass ratio of $\sim 1:1$) as the source and pieces of Si wafer covered with 10-nm-thick thermally evaporated Au catalysts as the substrates. The synthesis temperature was 850 °C. After the synthesis process, yellowish products were characterized using a field emission scanning electron microscope (FESEM) Amray 1910 FE and a high-resolution transmission electron microscope (HRTEM) Tecnai F30 equipped with an energy-dispersive x-ray (EDX) spectroscope. The electrical properties of the *p*-type Zn_3P_2 NWs were characterized by fabricating single NW MISFETs. The measurement results showed the average hole concentration and mobility at about 5.6×10^{16} cm^{-3} and 42.5 $cm^2/V \cdot s$, respectively.[21]

The MESFETs based on *p*-type Zn_3P_2 single NWs were fabricated as follows: First, the Zn_3P_2 NW suspension was dropped on oxidized Si substrates each with a SiO_2 layer of about 300 nm. Then, UV lithography, thermal evaporation, and lift-off processes were used to fabricate the source and

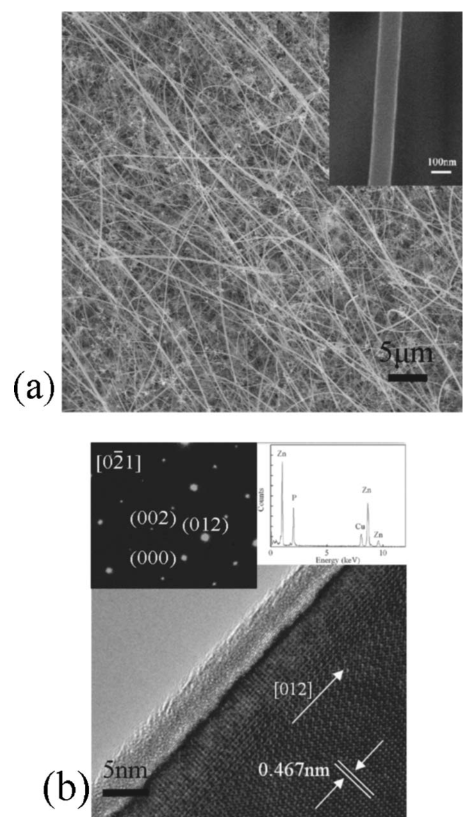

FIG. 1. (a) The FESEM image of as-synthesized Zn_3P_2 NWs. The inset is a magnified image that shows that the diameter of a typical Zn_3P_2 NW is about 100 nm. (b) The HRTEM image of a Zn_3P_2 NW. The inset at the upper-left corner is the corresponding SAED pattern. The inset at the upper-right corner is the EDX spectrum of the Zn_3P_2 NW.

[a)]Authors to whom correspondence should be addressed. Electronic addresses: lundai@pku.edu.cn, and qingg@pku.edu.cn.

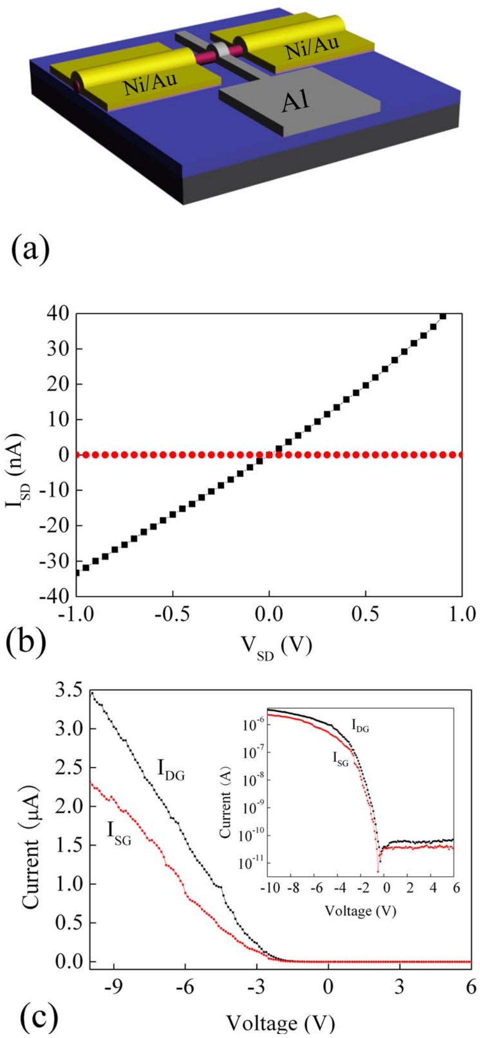

FIG. 2. (Color online) (a) The schematic illustration of the Zn_3P_2 single NW MESFET. (b) I_{SD}-V_{SD} curves before (the black line) and after (the red line) evaporating a top Al Schottky gate. (c) *I-V* curves between the source-gate and drain-gate, where the source or the drain was grounded. The inset is the *I-V* curves on an exponential scale.

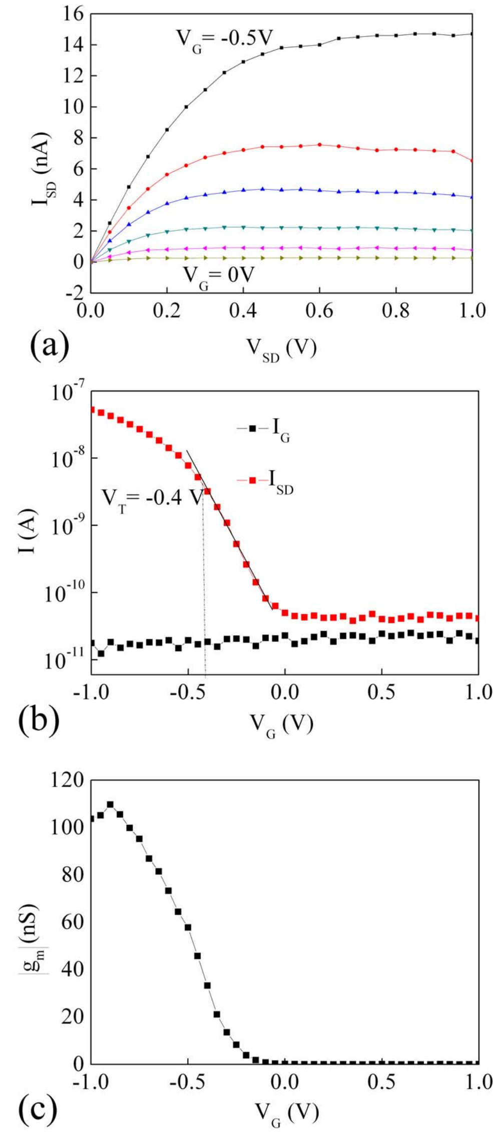

FIG. 3. (Color online) (a) I_{SD}-V_{SD} characteristics of a *p*-type Zn_3P_2 MESFET measured at room temperature under gate biases ranging from −0.5 to 0 V with a step of 0.1 V. (b) The I_{SD}-V_G (the red line) and I_G-V_G (the black line) curves of the MESFET measured at $V_{SD}=1$ V on an exponential scale. (c) The $|g_m|$-V_G curve at $V_{SD}=1$ V.

drain Ohmic contact Ni/Au (10 nm/90 nm thick) electrodes. Lastly, a similar process was used to make a top surrounding Schottky Al gate electrode (100 nm thick) across the NW between the source and drain electrodes. The electrical transport measurements on the *p*-type Zn_3P_2 MESFETs were conducted using a semiconductor characterization system (Keithley 4200).

III. RESULTS AND DISCUSSIONS

Figure 1(a) shows a typical FESEM image of as-synthesized *p*-type Zn_3P_2 NWs. The inset is a magnified FESEM image. Each Zn_3P_2 NW has a smooth surface and a uniform diameter along the growth direction. The average diameter of the NWs is about 100 nm, and the length is several tens of microns.

The inset at the upper-right corner of Fig. 1(b) is the EDX spectrum taken from a Zn_3P_2 NW. It consists of only Zn and *P* signals with an atomic ratio of about 3:2. Figure 1(b) shows the HRTEM image of the Zn_3P_2 NW. The crystal planes with a spacing distance of about 0.467 nm can be seen along the growth direction. According to Ref. 22, these planes can be indexed as the tetragonal Zn_3P_2 (012) planes. The inset at the upper-left corner of Fig. 1(b) is the corresponding selected area electron diffraction (SAED) pattern recorded along the $[0\bar{2}1]$ zone axis. The HRTEM image, together with the SAED pattern, reveals that the Zn_3P_2 NW is a single crystal with the tetragonal structure, and its growth direction is [012].

Figure 2(a) is a schematic illustration of the *p*-type Zn_3P_2 single NW MESFET. The gate length of the MESFET is about 3 μm. The space distance between the source and drain electrodes is about 40 μm.

Figure 2(b) shows the source-drain currents (I_{SD}) versus source-drain voltage (V_{SD}) before (the black line) and after (the red line) evaporating the top Al Schottky gate. Before evaporating the top Al Schottky gate, the $I_{SD}\sim V_{SD}$ relation is nearly a straight line, indicating the formation of quite good Ohmic contacts between the Ni/Au electrodes and the p-type Zn_3P_2 NW. From the I-V curve and the dimensions of the NW channel, the resistivity of the p-type Zn_3P_2 NW is obtained to be about 9.3 Ω cm. When a top Al Schottky gate was made, the p-type Zn_3P_2 NW channel was pinched off, and the I_{SD} was below several picoamperes.

Figure 2(c) shows I-V characteristics between the source-gate and drain-gate, where the source or the drain was grounded. The inset is the corresponding I-V characteristics on an exponential scale. We can see a good Schottky contact between the Al electrode and the p-type Zn_3P_2 NW. The on/off current ratio of the Schottky junction is larger than 10^4 when the gate bias changes from -10 to $+6$ V.

Figure 3(a) shows the I_{SD} vs V_{SD} curves at various gate biases (V_G) for the p-type Zn_3P_2 NW MESFET. We can see that the NW MEFET is turned off at zero gate bias. This means that the as-fabricated NW MEFET is in the E-mode. Besides, for a given V_{SD}, I_{SD} decreases sharply when V_G increases from -0.5 to 0 V, indicating the p-type conductance characteristic of the NW.

Figure 3(b) shows the I_{SD} vs V_G (the red line) and gate leakage current (I_G) vs V_G (the black line) relations on an exponential scale measured at $V_{SD}=1$ V. In our case, V_G is limited to be above -1 V to avoid excessive I_G leakage. From the I_{SD}-V_G curve, an on/off current ratio can be obtained to be about 10^3 when V_G changes from -1 to 1 V. The threshold gate voltage (V_T) obtained is about -0.4 V.

Figure 3(c) shows the absolute value of the transconductance ($g_m=dI_{SD}/dV_G$) vs the V_G curve. The maximum absolute value of transconductance is obtained to be about 110 nS at $V_G=-0.9$ V.

IV. CONCLUSION

In conclusion, we report p-type Zn_3P_2 single NW MESFETs for the first time. A top surrounding Al Schottky contact gate was made. The p-type Zn_3P_2 single NW MESFET works in the E-mode. The on/off ratio is about 10^3, the threshold voltage is about -0.4 V, and the maximum transconductance is about 110 nS.

ACKNOWLEDGMENTS

This work was supported by the National Natural Science Foundation of China (Grant Nos. 60576037, 10774007, 10574008, and 50732001) and by the National Basic Research Program of China (Grant Nos. 2006CB921607 and 2007CB613402).

[1] Z. Zhong, F. Qian, D. Wang, and C. M. Lieber, Nano Lett. **3**, 343 (2003).
[2] M. Law, D. J. Sirbuly, J. C. Johnson, J. Goldberger, R. J. Saykally, and P. D. Yang, Science **305**, 1269 (2004).
[3] T. Gao, Q. H. Li, and T. H. Wang, Appl. Phys. Lett. **86**, 173105 (2005).
[4] A. Pan, D. Liu, R. Liu, F. Wang, X. Zhu, and B. Zou, Small **1**, 980 (2005).
[5] J. S. Jie, W. J. Zhang, Y. Jiang, X. M. Meng, Y. Q. Li, and S. T. Lee, Nano Lett. **6**, 1887 (2006).
[6] W. Q. Yang, H. B. Huo, L. Dai, R. M. Ma, S. F. Liu, G. Z. Ran, B. Shen, C. L. Lin, and G. G. Qin, Nanotechnology **17**, 4868 (2006).
[7] H. Y. Cha, H. Q. Wu, S. Chae, and M. G. Spencer, J. Appl. Phys. **100**, 024307 (2006).
[8] A. Ponzoni, E. Comini, G. Sberveglieri, J. Zhou, S. Z. Deng, N. S. Xu, Y. Ding, and Z. L. Wang, Appl. Phys. Lett. **88**, 203101 (2006).
[9] Q. Wan, E. N. Dattoli, and W. Lu, Appl. Phys. Lett. **90**, 222107 (2007).
[10] G. Jo, J. Maeng, T. W. Kim, W. K. Hong, B. S. Choi, and T. Lee, J. Appl. Phys. **102**, 084508 (2007).
[11] Y. Huang, X. Duan, Y. Cui, and C. M. Lieber, Nano Lett. **2**, 101 (2002).
[12] Y. Cui, Z. Zhong, D. Wang, W. U. Wang, and C. M. Lieber, Nano Lett. **3**, 149 (2003).
[13] S. Ju, K. Lee, D. B. Janes, M. H. Yoon, A. Facchetti, and T. J. Marks, Nano Lett. **5**, 2281 (2005).
[14] J. S. Jie, W. J. Zhang, Y. Jiang, and S. T. Lee, Appl. Phys. Lett. **89**, 223117 (2006).
[15] J. Goldberger, A. I. Hochbaum, R. Fan, and P. Yang, Nano Lett. **6**, 973 (2006).
[16] K. Keem, D. Y. Jeong, S. Kim, M. S. Lee, I. S. Yeo, U. I. Chung, and J. T. Moon, Nano Lett. **6**, 1454 (2006).
[17] J. Xiang, W. Lu, Y. Hu, Y. Wu, H. Yan, and C. M. Lieber, Nature (London) **441**, 489 (2006).
[18] W. I. Park, J. S. Kim, G. C. Yi, and H. J. Lee, Adv. Mater. (Weinheim, Ger.) **17**, 1393 (2005).
[19] R. M. Ma, L. Dai, and G. G. Qin, Appl. Phys. Lett. **90**, 093109 (2007).
[20] R. M. Ma, L. Dai, and G. G. Qin, Nano Lett. **7**, 868 (2007).
[21] C. Liu, L. Dai, L. P. You, W. Q. Yang, R. M. Ma, Y. F. Zhang, and G. G. Qin, J. Mater. Chem., 2008 (unpublished).
[22] JCPDS Card No. 65-2854.